Citation: Simborio, T., T. Yokoi, T. Hara (2022), Strong ground motion simulation of the 2020 Masbate, Philippines earthquake (Mw6.6) using Empirical Green's Function method, Synopsis of IISEE-GRIPS Master's Thesis.

STRONG GROUND MOTION SIMULATION OF THE 2020 MASBATE, PHILIPPINES EARTHQUAKE (M_w6.6) USING EMPIRICAL GREEN'S FUNCTION METHOD

Tom Carlo E. Simborio[1] **Supervisor: Toshiaki YOKOI**[2] **, Tatsuhiko HARA**[3]
MEE21705

ABSTRACT

Strong ground motions of the August 18, 2020 Mw 6.6 Masbate, Philippines earthquake were simulated using the August 11, 2020 Mw 4.9 Masbate, Philippines earthquake records of the Philippine Strong Motion Network through the Empirical Green's Function (EGF) method. The fault dimensions and stress drop ratios were calculated through the source spectral fitting method. A grid search was done to obtain a set of parameters for the EGF method that explains the observed strong motion data well. These parameters include the rupture starting point, rupture velocity, rise time, length, and width of the strong motion generation area (SMGA). The result suggests the rupture started in the shallow southern segment of the fault plane. The peak ground accelerations (PGAs) from the simulated waveforms are consistent with the observed PGAs, and a directivity effect was also simulated. The PGAs calculated using a ground motion prediction equation used for hazard estimations in the Philippines overestimates for three stations among the four stations analyzed in this study. The peak ground displacements (PGDs) from the simulated waveforms are underestimates compared to the observed PGDs. The ratio of the size of the SMGA to the moment magnitude and the ratio of the rise time to the moment magnitude are smaller than those obtained in previous studies.

Keywords: Strong Ground Motion, Empirical Green's Function Method, Peak Ground Acceleration.

1. INTRODUCTION

The Philippines experiences earthquakes every day due to its geotectonic setting. Within the country is the Philippine Fault Zone (PFZ) that transects the entire country and divided into segments. One of its segments is the Masbate segment. Significant earthquakes occurred in the history of Masbate; one damaging earthquake occurred on August 18, 2020, with a moment magnitude M_w 6.6.

As of November 2021, the Philippines has 103 strong-motion stations throughout the country. Recorded events are analyzed, cataloged, and stored in a database for scientific research, especially in earthquake engineering, to update the National Structural Code in the Philippines (Grutas et al., 2017).

The objective of this study is to investigate the applicability of the Empirical Green's Function (EGF) method to the current strong ground motion data of the Philippine Strong Motion Network (PSMNet). Specifically, I conducted the following: I estimated the parameters for the strong motion generation area and compared them to those obtained by previous studies. I compared the peak ground accelerations (PGAs) from the EGF simulations to the observed PGAs and compared the peak ground displacements (PGDs) from the EGF simulations to the observed PGDs. I also compared the PGAs from the EGF simulations to the computed PGAs based on the ground motion prediction equation (GMPE) by Fukushima and Tanaka (1990, 1992).

2. METHODOLOGY

[1] Department of Science and Technology-Philippine Institute of Volcanology and Seismology (DOST-PHIVOLCS), Philippines
[2] Japan International Cooperation Agency (JICA)
[3] International Institute of Seismology and Earthquake Engineering, Building Research Institute (IISEE-BRI)

2.1. Empirical Green's Function (EGF) method

Empirical Green's Function (EGF) is a method to synthesize waveforms of a large event, which is referred to as a target event, using seismograms recorded from a smaller event, which is referred to as an element event (e.g., Irikura, 1986; Irikura et al.; 1997; Miyake et al., 2003). In the EGF method, the fault plane of the target event is divided into NxN subfaults, and the subfault corresponds to the size of the fault plane of the element event. The waveform of a target event, U(t), is calculated by:

$$U(t) = \sum_{i=1}^{N}\sum_{j=1}^{N}\frac{r}{r_{ij}}\,F(t) * [C \cdot u(t)] \quad (1)$$

where U(t) is the synthetic waveform of the target event; i and j are indices of the subfaults; r is the hypocentral distance from the element event to the recording stations; r_{ij} is the distance from recording stations to each subfaults; F(t) is the Modified Filtering (Correction) function; C is the ratio of the stress drops between the element and target events, and u(t) is the observed waveform of the element event. The Modified Filtering function F(t) by Irikura et al. (1997) is used.

2.2. Source spectral fitting method

As stated above, the parameters N and C are necessary to perform the EGF method. Miyake et al. (1999) proposed the source spectral fitting method to determine N and C parameters objectively. This method fits the average of the observed spectral ratio between the target and element events to a theoretical source spectral ratio to estimate $\left(\frac{M_o}{m_o}\right)$, corner frequencies of the target event (f_{cm}) and element event (f_a), where M_o and m_o are the seismic moments of the target and element events, respectively.

For calculations of observed source spectra, I set V_s to 3.2 km/s and used $Qs(f) = 105.02f^{0.75}$ which Oestar and Hayashida (2021) obtained. I minimized the sum of the squared differences between the average of the observed spectral ratio and to a theoretical source spectral ratio over a frequency range, while Miyake et al. (1999) took the standard deviations of the observed spectral ratio into account. The minimization is conducted by a heuristic method introduced by Press et al. (1992), which combined the Down Hill Simplex Method (Nelder and Mead, 1965) and the Very Fast Simulated Annealing (Ingber, 1989). N and C are calculated by:

$$N = \frac{f_{ca}}{f_{cm}} \quad (2)$$

$$C = \left(\frac{M_o}{m_o}\right)\left(\frac{f_{cm}}{f_{ca}}\right)^3 \quad (3)$$

2.3. Grid search

After the values of N and C are obtained, the grid search is carried out to find parameters of the EGF to explain the observed strong ground motion records well. This method is done by initially setting parameters for the position of rupture starting point, rupture velocity, a rise time, the length, and width of the subfaults; executing EGF, and calculating residuals. The misfit function to be minimized is:

$$\text{Residual} = \sum_{\text{Station}}\sum_{\text{Component}}\left\{\frac{\frac{\sum_{i=1}^{N}(U_{obs}-U_{syn})^2}{\left(\sum_{i=1}^{N}U_{obs}^2\cdot\sum_{i=1}^{N}U_{syn}^2\right)^2}+5\cdot\left[\frac{\sum_{i=1}^{N}(A_{env.\,obs}-A_{env.\,syn})^2}{\left(\sum_{i=1}^{N}A_{env.\,obs}^2\cdot\sum_{i=1}^{N}A_{env.\,syn}^2\right)^2}\right]}{6}\right\} \quad (4)$$

where U_{obs} and U_{syn} are the observed and synthetic displacement, respectively; $A_{env.\,obs.}$ and $A_{env.\,syn.}$ are the envelopes of the observed and synthetic acceleration, respectively.

I put a larger weight for the differences of the acceleration envelopes, because the differences of the displacements are larger. I determined the weight in Eq. (4) after trying several different weights.

3. DATA

3.1. Earthquake parameters

Two earthquakes are necessary to perform the Empirical Green's Function (EGF) method: a target event (mainshock) and an element event – a smaller event that occurred in the vicinity of the mainshock. Through inspection, I selected the August 11, 2020 event ("08/11/2020 – 0726Z" in Figure 1), which is nearest to the mainshock ("08/18/2020 – 0003Z" in Figure 1) among the earthquake events as the element event. The distance between the foreshock and mainshock is approximately 4 km. The earthquake source parameters of the target and element events are summarized in Table 1. The second nodal plane (NP2) was used in this study based on the surface rupture and aftershock distribution.

Table 1. The origin times, hypocenters, magnitudes, and the focal mechanisms of the element and target events. The origin times and hypocenters are from the earthquake catalog of the DOST-PHIVOLCS. The magnitudes and focal mechanisms are from the moment tensors solutions from the SWIFT system (https://swift1.phivolcs.dost.gov.ph/).

	Date	Time (UTC)	Latitude (N°)	Longitude (E°)	Depth (km)	Magnitude (M_w)	NP	Strike (°)	Dip (°)	Rake (°)
Element Event	08/11/2020	07:26:41.23	11.943	124.055	13.2	4.9	NP1	231	85	177
							NP2	321	87	5
Target Event	08/18/2020	00:03:46.79	11.969	124.027	11.4	6.6	NP1	235	64	-174
							NP2	142	85	-26

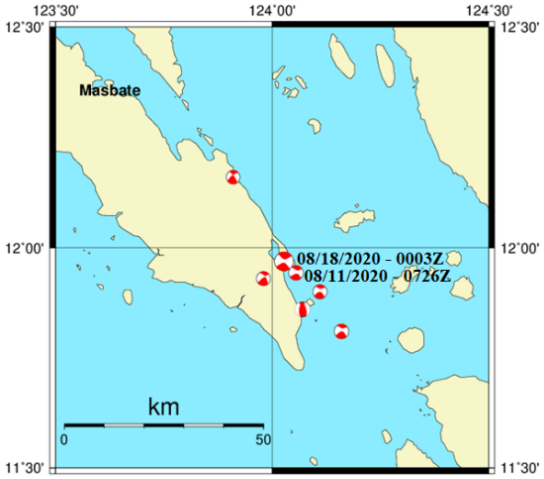

Figure 1. Moment tensor solutions of the 2020 Cataingan, Masbate earthquake, and its foreshocks and aftershocks.

Figure 2. Station distribution of accelerometers that recorded the foreshock and mainshock.

3.2. Strong motion records of the foreshock and mainshock and data preparation

Twenty Kinemetrics ETNA-2 accelerometers of the PSMNet recorded both the foreshock and mainshock. I used four stations since data from at least four stations are necessary to perform EGF calculations (Miyake et al., 2003). I chose the closest stations in Masbate, Bicol Region, Leyte Island, and Cebu Province (MMPA, BCPL, LYKN, and CLIL, respectively) from the events (Figure 2). The recorded waveforms are saved as an Event Log file. These records are converted to ASCII files using the ViewWave software (Kashima, 2022) and are converted into files in the KNET format (https://www.kyoshin.bosai.go.jp/kyoshin/man/knetform_en.html). I added appropriate headers to the KNET format files and obtained ZOO format files. Data in the ZOO format are necessary to perform Empirical Green's Function method.

I used a time series starting from 8 seconds before the theoretical P-arrival time, whose duration is 81.92 seconds. I manually picked an S-arrival time using a strong motion record and its Husid plot (Husid, 1969). A cosine taper function in which the value of the function becomes one at the S-arrival time is multiplied to the strong motion data. The tapered part is extracted and used in this study.

I used the vector sum, which is the square root of the sum of the squares of the acceleration amplitude spectra of the horizontal components. Parzen window was used to smoothen the acceleration amplitude spectra to reduce the oscillatory behavior of the spectra.

4. RESULTS AND DISCUSSION

4.1. Source spectral fitting

Figure 3 shows the result of the source spectral ratio fitting. The thick theoretical curve shows the frequency range used for fitting. I used the average of the source spectra ratios in the frequency range from 0.2 to 8 Hz for source spectra ratio fitting. The low-frequency asymptote is 0.01, whereas the high-frequency asymptote is 0.2. The corner frequency of the mainshock is 0.33 Hz, whereas the corner frequency of the foreshock is 1.33 Hz. From Eq. (2) and (3), it can be calculated that the ratio of fault dimensions (N) is 4, and the ratio of the stress drop between the events (C) is 1.56.

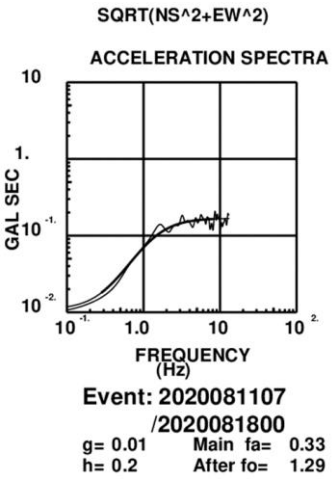

Figure 3. The result of the source spectral ratio fitting.

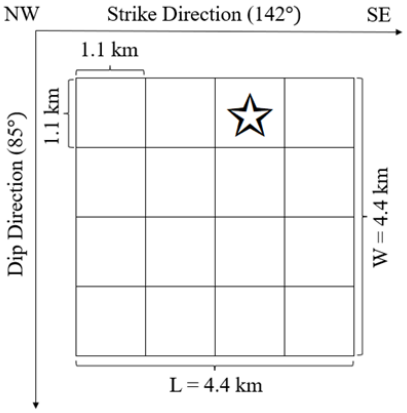

Figure 4. Schematic illustration of the strong motion generation area of the August 18, 2020, Masbate, Philippines earthquake. The star represents the rupture starting point.

4.2. Grid search

I performed a grid search for parameters of the EGF method. The parameters searched in this study are the position of rupture starting point, rupture velocity, a rise time, and the length and width of the subfaults. Based on the model parameters that minimize the misfit function defined in Eq. (4), the strike of the rupture is well-constrained at position 3, the dip is at position 1, the rupture velocity is 3.0 km/s, the rise time is 0.05 s, length, and width of the subfaults are 1.1 km. Figure 4 shows a schematic illustration of the strong motion generation area of the August 18, 2020, Masbate, Philippines earthquake where the star denotes the rupture starting point. The result suggests that the rupture started at the shallow southern segment of the fault plane.

4.3 Empirical Green's Function simulation, peak ground accelerations (PGAs), and peak ground displacements (PGDs)

Synthetic seismograms of the target event were computed by the EGF method using the set of parameters obtained by the grid search method. An example is shown in Figure 5. The observed and synthetic acceleration waveforms are similar to each other. The differences between the displacement waveforms are large.

Figure 6 shows the comparison of the different PGAs. I compared the observed PGAs with the synthetic PGAs and PGAs obtained from the ground motion prediction equation (GMPE) by Fukushima and Tanaka (1990, 1992). I also compared the observed PGDs with the synthetic PGDs. Comparing the observed PGAs to the synthetic PGAs, they are comparable. Comparing the observed PGA to the PGA computed by the GMPE, the latter overestimate for three of the four stations analyzed in this study. In terms of PGDs (Figure 7), the synthesized PGDs tend to underestimate.

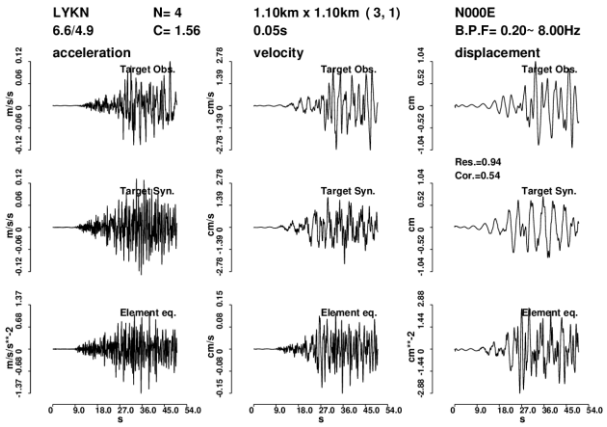

Figure 5. The observed and synthetic waveforms of LYKN (N-S)

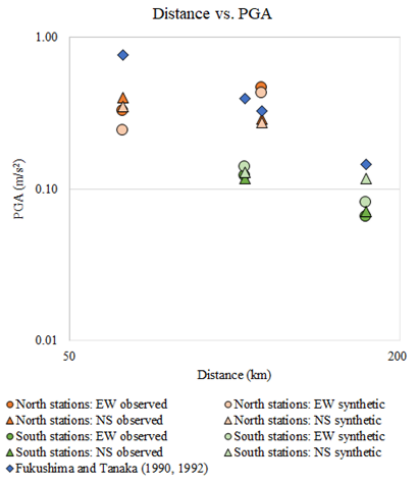

Figure 6. Comparison of the observed PGAs and the calculated PGAs.

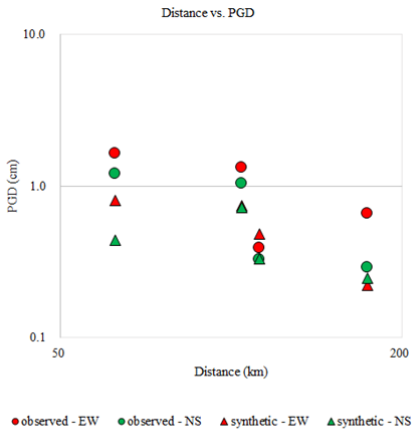

Figure 7. Comparison of the observed PGDs and calculated PGDs.

4.4 Source scaling

I compared the results of this study to the empirical source scaling relationships for crustal earthquakes by Sommerville et al. (1999) and Miyake et al. (2003). The comparison is made by comparing the moment magnitude with the SMGA size (Figure 8 (a)) and with the rise time (Figure 8 (b)). For the moment magnitude of 6.6 of the 2020 Masbate earthquake, the SMGA size and rise time are smaller than the general trends of the previous studies.

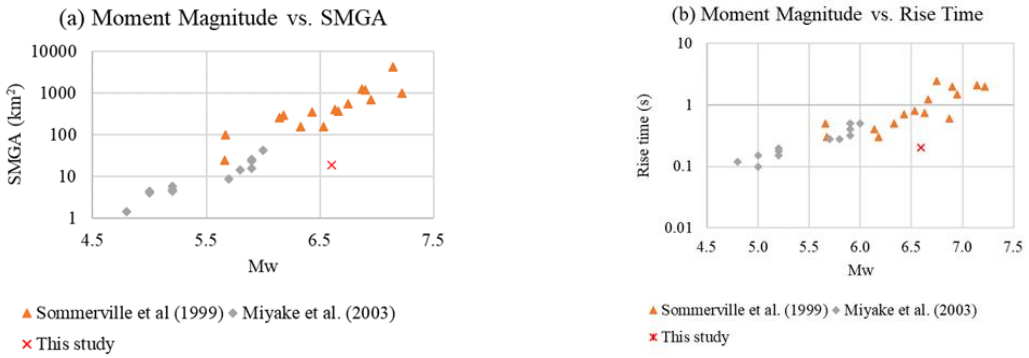

Figure 8. Comparison of the moment magnitude to (a) SMGA and (b) rise time.

5. CONCLUSIONS

This study has shown the applicability of the Empirical Green's Function (EGF) method to the current strong ground motion data of the Philippine Strong Motion Network (PSMNet). The parameters for the strong motion generation area (SMGA) were estimated through grid search. The result suggests that the rupture started in the southern segment of the fault plane, and the rupture is shallow. The peak ground accelerations (PGAs) from the EGF simulations to the observed PGAs were comparable, and the observed effect of the directivity is reproduced. The PGAs from the EGF simulations were compared to the computed PGAs based on the ground motion prediction equation (GMPE) by Fukushima and Tanaka (1990, 1992), and it shows the PGAs calculated using the aforementioned GMPE tend to overestimate. The peak ground displacements (PGDs) from the EGF simulations to the observed PGDs tend to underestimate. Compared to previous studies, it shows the size of the SMGA and rise time is smaller. Further applications will help examine the source characteristics of earthquakes in and around the Philippines.

ACKNOWLEDGEMENTS

This research was conducted as an individual study for the training course "Seismology, Earthquake Engineering, and Tsunami Disaster Mitigation" by IISEE-BRI, JICA, and GRIPS. I sincerely thank Dr. Toshiaki Yokoi and Dr. Tatsuhiko Hara for supervising me. I thank Dr. Irikura and Dr. Miyake for their lectures on Strong Ground Motion Study and the Empirical Green's Function program. I also thank the DOST-PHIVOLCS for nominating me for this opportunity and assisting in my data requests. I used the Seismic Analysis Code (SAC, Goldstein et al., 2003; Goldstein and Snoke, 2005) in some parts of the data processing in this study. The Generic Mapping Tools (GMT, Wessel and Smith, 1998) was used to make a figure in this study.

REFERENCES

Goldstein, P., Dodge, D., Firpo, M., Minner, L., 2003, edited by Lee, WHK, Kanamori, H., Jennings, P.C., and Kisslinger, C., Academic Press, London.

Goldstein, P., Snoke, A., 2005, Incorporated Institutions for Seismology Data Management Center Electronic Newsletter.

Grutas, R., Tiglao, R., Lasala, M., Deocampo, J., Narag, I., and Solidum Jr., R.U., 2017, IAG-IASPEI.

Fukushima, Y., and Tanaka, T., 1990, Bull. Seism. Soc. Am., 80, 757-783.

Fukushima, Y., and Tanaka, T., 1992, The Seismological Society of Japan 1992 Fall Meeting.

Husid, L.R., 1969, Características de Terremotos, Análisis General, Revista del IDIEM 8, Santiago, Chile, 21–42.

Ingber, L., 1989, Mathematical and Computer Modelling, 12, 967-973

Irikura, K., 1986, Proceedings of the 7th Japan earthquake engineering symposium, 151–156.

Irikura, K., Kagawa, T., and Sekiguchi, H., 1997, Seism. Soc. Japan 2, B25 (in Japanese).

Kashima, T., 2022, ViewWave (version 2.2.6), http://smo.kenken.go.jp/~kashima/viewwave.

Miyake, H., Iwata, T., & Irikura, K., 1999, Zisin, 51, 431–442. (in Japanese with English abstract).

Miyake, H., Iwata, T., and Irikura, K., 2003, Bull. Seis. Soc. Am., 93, 2531 – 2545.

Nelder, J. A., and Mead R., 1965, The Computer Journal, 7, 4, 308–313

Oestar, J., and T. Hayashida, 2021, Synopsis of IISEE-GRIPS Master's Thesis.

Press, W.H., Teukolsky, S.A., Vetterling, W.T., and Flannery, B.P., 1992, Cambridge University Press, USA.

Somerville, P., Irikura, K., Graves, R., Sawada, S., Wald, D., Abrahamson, N., Iwasaki Y., Kagawa T., Smith, N., Kowada, A., 1999, Seismological Research Letters, 70, 59–80.

Wessel, P., and Smith, W.H.F., 1998, New, improved version of Generic Mapping Tools released, Eos, Trans. AGU, 79, 579, 1998